

Supporting Information
for
Hydrogels with Both Mechanical Strength and Luminescence
Anisotropy

*Xiao Liu,^a Bin Li,^a Wenjing Wang,^a Zhiqiang Li^{*a} and Qingqing Xiong^{*b}*

^aTianjin Key Laboratory of Chemical Process Safety, School of Chemical Engineering and Technology, Hebei University of Technology, Guangrong Dao 8, Hongqiao District, Tianjin 300130, P. R. China. Email: zhiqiangli@hebut.edu.cn

^b Department of Hepatobiliary Cancer, Liver Cancer Research Center for Prevention and Therapy, Tianjin Medical University Cancer Institute & Hospital, National Clinical Research Center for Cancer; Key Laboratory of Cancer Prevention and Therapy, Tianjin; Tianjin's Clinical Research Center for Cancer; Tianjin 300060, P. R. China. E-mail: xionqingqing@tmu.edu.cn

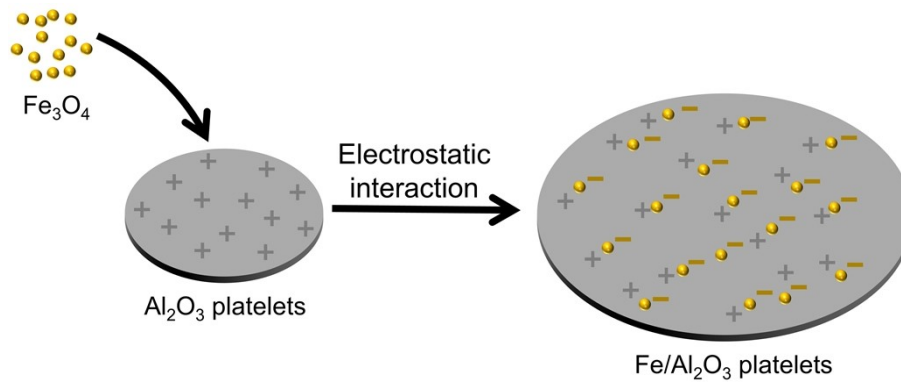


Figure S1. Preparative route of Fe/Al₂O₃ platelets.

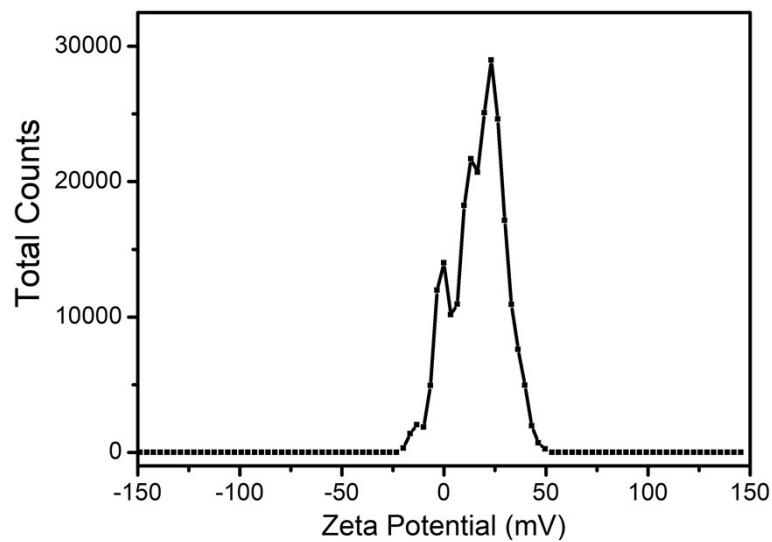


Figure S2. Zeta potential of pristine Al₂O₃ platelets in deionized water ($\zeta = 16.9$ mV).

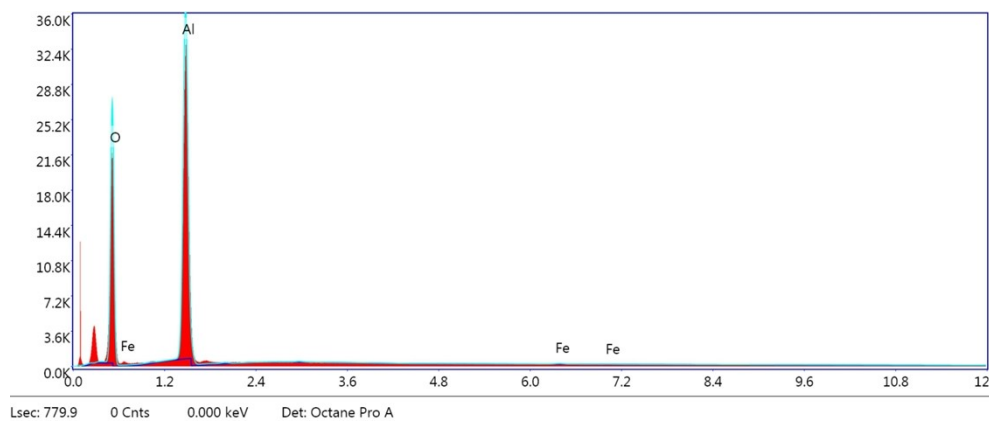


Figure S3. EDS spectrum of Fe/Al₂O₃ platelets.

Table S1. Elemental composition of Fe/Al₂O₃ platelets.

Element	Weight %	Atomic %
O	50.38	63.25
Al	49.13	36.58
Fe	0.49	0.18

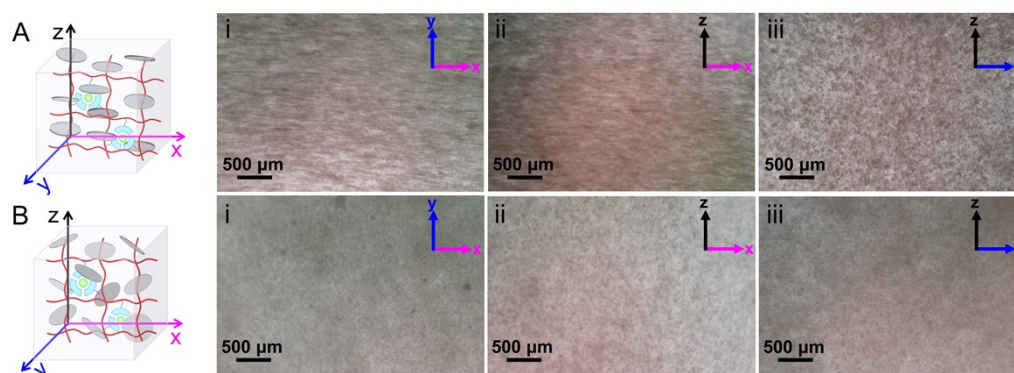


Figure S4. Optical microscope images of Tb-containing hydrogel in different directions.

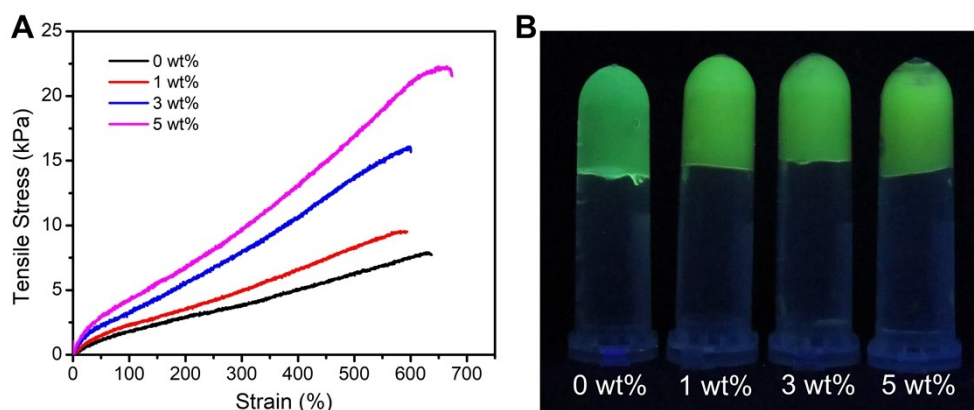
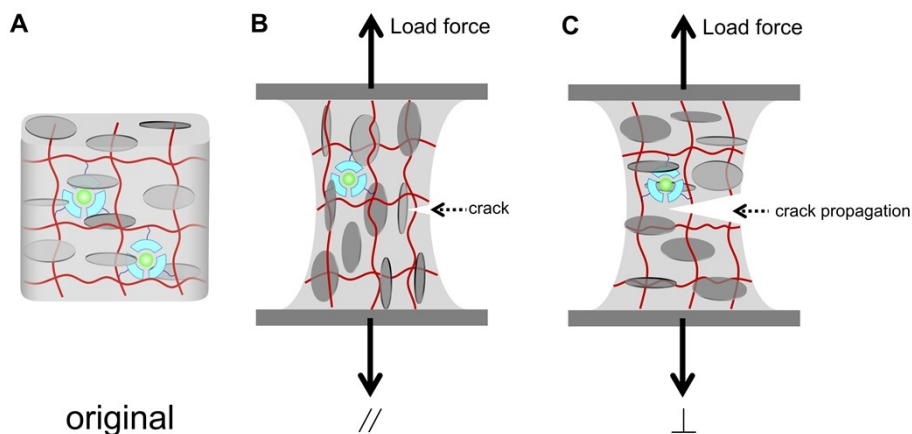
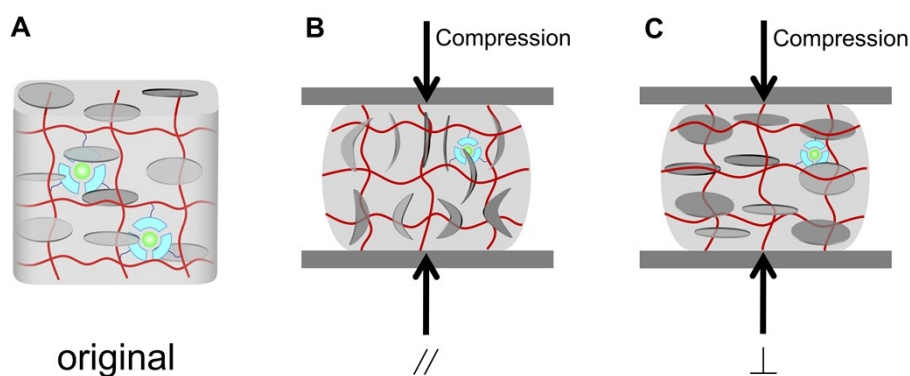


Figure S5. (A) Tensile stress-strain and (B) photos (under 254 nm UV light) of Tb-containing hydrogel with different contents of Fe/Al₂O₃ platelets.



Scheme S1. Schematic illustration of Tb-containing hydrogel (A) original, tensile force was (B) parallel and (C) perpendicular to the oriented Fe/Al₂O₃ platelets.



Scheme S2. Schematic illustration of Tb-containing hydrogel (A) original, compressive force was (B) parallel and (C) perpendicular to the oriented Fe/Al₂O₃ platelets.

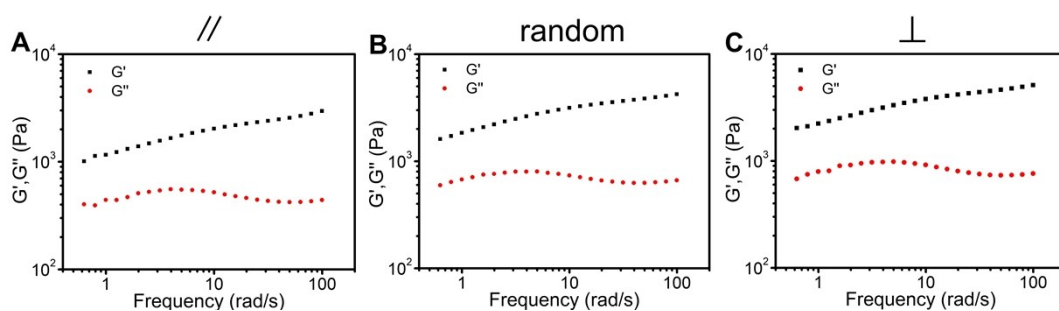


Figure S6. Frequency (ω) sweep tests at $\omega = 0.1-100 \text{ rad s}^{-1}$ and strain (γ) = 1.0% of Tb-containing hydrogel.

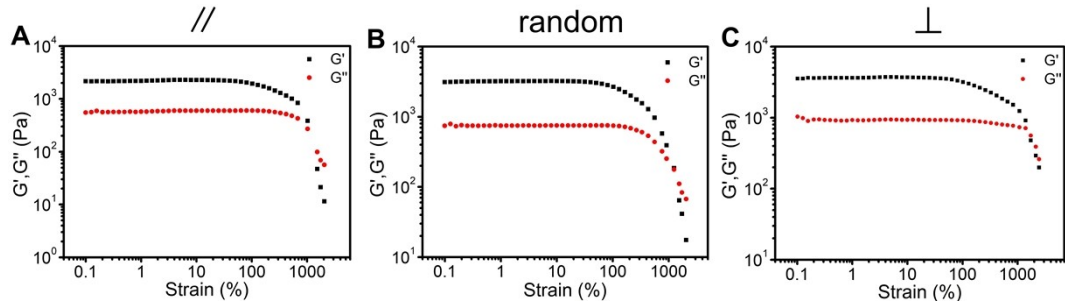


Figure S7. Strain sweep tests at $\gamma = 0.1$ -2000% with $\omega = 1.59$ Hz of Tb-containing hydrogel.

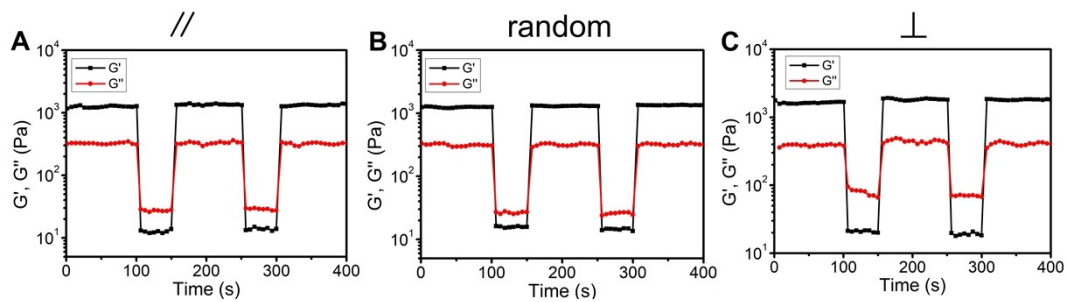


Figure S8. Continuous step strain test of Tb-containing hydrogel at $\gamma = 0.1$ and 800% with $\omega = 1.59$ Hz.

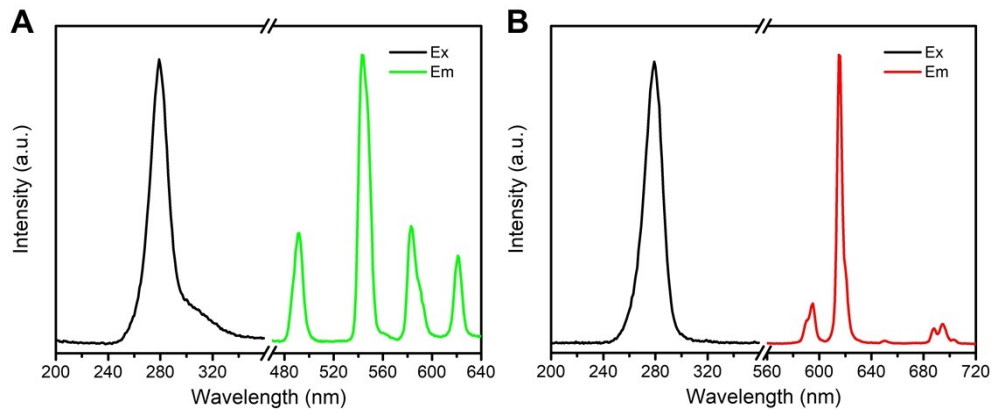


Figure S9. Normalized excitation ($\lambda_{\text{mon}} = 544$ nm for Tb, 615 nm for Eu) (left) and emission ($\lambda_{\text{ex}} = 280$ nm) (right) luminescence spectra of (A) Tb-containing and (B) Eu-containing hydrogel.

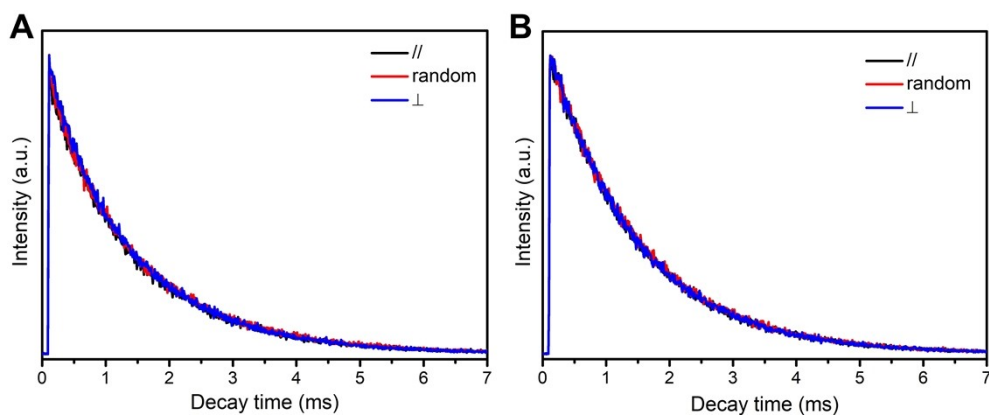


Figure S10. Decay curves of (A) Tb-containing (excited at 280 nm and monitored at 544 nm) and (B) Eu-containing (excited at 280 nm and monitored at 615 nm) hydrogel along different direction.

Table S2. Luminescence quantum efficiency (Φ) and lifetime (τ) of Tb-containing and Eu-containing hydrogel.

Sample		//	random	⊥
Tb-containing hydrogel	τ (ms)	1.33	1.36	1.31
	Φ (%)	4.87	4.91	4.40
Eu-containing hydrogel	τ (ms)	1.41	1.43	1.40
	Φ (%)	13.04	12.28	12.55